Journal of Organometallic Chemistry, 315 (1986) 255–268
Elsevier Sequoia S.A., Lausanne – Printed in The Netherlands

HALOALKYL COMPLEXES OF THE TRANSITION METALS

IV *. THE FORMATION OF A CATIONIC YLIDE COMPLEX OF PLATINUM(II) FROM A CHLOROMETHYLPLATINUM(II) COMPLEX AND THE CRYSTAL STRUCTURES OF *cis*-[Pt(CH_2PPh_3)X(PPh_3)$_2$]I (X = Cl or I)

CAROLA ENGELTER, JOHN R. MOSS **, LUIGI R. NASSIMBENI, MARGARET L. NIVEN,
GORDON REID and JOHN C. SPIERS

School of Chemical Sciences, University of Cape Town, Rondebosch 7700 (South Africa)

(Received May 6th, 1986)

Summary

The reactions of Pt(PPh_3)$_4$ and Pt(C_2H_4)(PPh_3)$_2$ with CH_2ClI have been investigated. The product of the reaction of Pt(PPh_3)$_4$ with CH_2ClI is the cationic ylide complex *cis*-[Pt(CH_2PPh_3)Cl(PPh_3)$_2$][I], whereas the reaction of Pt(C_2H_4)(PPh_3)$_2$ gives the oxidative addition product Pt(CH_2Cl)I(PPh_3)$_2$. Reaction of *cis*- or *trans*-[Pt(CH_2Cl)I(PPh_3)$_2$] with PPh_3 gives the complex *cis*-[Pt(CH_2PPh_3)Cl(PPh_3)$_2$][I]. The structures of the complexes *cis*-[Pt(CH_2PPh_3)X(PPh_3)$_2$][I] (where X = Cl or I) have been determined by X-ray crystallography. Both complexes crystallize in the monoclinic space group $P2_1/n$. For X = Cl *a* 1388.6(7), *b* 2026.7(10), *c* 1823.9(9) pm, *β* 96.51(2)° and *R* converged to 0.075 for 3542 observed reflections; structural parameters Pt–Cl 240(1), Pt–C(3) 212(2), Pt–P(2) (*trans* to Cl) 235(1) and Pt–P(1) (*trans* to CH_2PPh_3) 233(1) pm; Cl–Pt–C(3) 86.9(5), C(3)–Pt–P(2) 91.8(5), P(2)–Pt–P(1) 97.0(2) and P(1)–Pt–Cl 85.1(2)°. For X = I, *a* 1379.4(7), *b* 2044.4(10), *c* 1840.0(9) pm, *β* 96.09(2)° and *R* converged to 0.071 for 4333 observed reflections; structural parameters Pt–I 266(1), Pt–C(3) 212(2), Pt–P(2) (*trans* to I) 226(1) and Pt–P(1) (*trans* to CH_2PPh_3) 233(1) pm; I–Pt–C(3) 87.2(5), C(3)–Pt–P(2) 91.5(5), P(2)–Pt–P(1) 96.5(2) and P(1)–Pt–I 85.6(1)°. Some other complexes of the type *cis*-[Pt(CH_2PPh_3)X(PPh_3)$_2$]Y are also described.

Introduction

The oxidative addition reaction of alkyl halides to zerovalent platinum compounds provides a common route for the synthesis of platinum(II) alkyl complexes

---

* For Part III see Ref. 12.

** Author to whom correspondence should be addressed.

[1]. A possible route to halomethyl complexes of platinum(II) would be via the reaction of a polyhalomethane with a zerovalent platinum complex. Reports of the reaction of $Pt(PPh_3)_4$ with CCl_4 however gave only $PtCl_2(PPh_3)_2$ [2]. More recently, it has been reported that dihalomethanes can oxidatively add to platinum(0) ethylene complexes with the formation of haloalkyl complexes [3–7]. For example:

$$Pt(C_2H_4)(PPh_3)_2 + CH_2Cl_2 \xrightarrow{h\nu} \textit{cis- and trans-}[Pt(CH_2Cl)Cl(PPh_3)_2] \qquad [3]$$

$$Pt(C_2H_4)(PEt_3)_2 + CH_2I_2 \rightarrow \textit{trans-}[Pt(CH_2I)I(PEt_3)_2] \qquad [6]$$

$$Pt(C_2H_4)(PPh_3)_2 + CH_2ClI \rightarrow \textit{cis-}[Pt(CH_2Cl)I(PPh_3)_2] \qquad [7]$$

As part of a general study of haloalkyl complexes of transition metals, we were interested in investigating routes to halomethyl complexes of platinum(II). We now report in detail on the reactions of $Pt(PPh_3)_4$ and $Pt(C_2H_4)(PPh_3)_2$ with CH_2ClI. We have already reported some aspects of this work [7,8].

Results and discussion

The reaction of $Pt(PPh_3)_4$ with CH_2ClI in benzene (see Scheme 1) gave a white crystalline compound in high yield. This compound can be formulated as the cationic ylide complex *cis*-$[Pt(CH_2PPh_3)Cl(PPh_3)_2][I]$ (I) on the basis of microanalysis, NMR, IR and conductivity data. Transition metal ylide complexes are now well-known [9]. Similar to the above reaction is the report of the reaction of $Pt(PEt_3)_3$ with CH_2I_2 which gave the ylide complex *trans*-$[Pt(CH_2PEt_3)I(PEt_3)_2][I]$ [10].

The metathetical replacement reaction of I with NaI gives *cis*-$[Pt(CH_2PPh_3)I(PPh_3)_2][I]$ (II). Other similar metathetical replacement reactions were also carried out, as were reactions to replace the counter anion. Difficulties were experienced in obtaining complete characterisation data on these derivatives of I and II, and they have therefore not been included in this paper; the difficulties with the microanalytical data are probably a result of varying amounts of solvent of crystallization with the samples.

Two possible mechanisms for the formation of I are: (a) via the oxidative addition of the phosphonium salt $[Ph_3PCH_2Cl][I]$ to the coordinatively unsaturated $Pt(PPh_3)_2$ or (b) via the complex $Pt(CH_2Cl)I(PPh_3)_2$ (III). We find that on addition of a concentrated solution of CH_2ClI to a saturated benzene solution of $Pt(C_2H_4)(PPh_3)_2$, an almost white crystalline product is rapidly precipitated. This product we believe to be *cis*-$[Pt(CH_2Cl)I(PPh_3)_2]$ (IIIa) and we assign this stereochemistry largely on the basis of ^1H and ^{31}P NMR data. The product is mainly *cis*-$[Pt(CH_2Cl)I(PPh_3)_2]$ but traces of the *trans*-isomer are observed in some samples. Use of concentrated solutions and short reaction times maximizes the yield of the *cis*-isomer. This is in agreement with further experiments where we show that IIIa can be isomerized to IIIb in solution. Thus, *cis*-$[Pt(CH_2Cl)I(PPh_3)_2]$ can be completely isomerised to the *trans*-isomer by refluxing IIIa or a mixture of IIIa and IIIb, in benzene for 1 h. This isomerisation of IIIa to IIIb occurs more slowly in solution at room temperature and was followed by both ^1H and ^{31}P NMR. The ^1H NMR spectrum of IIIa shows a doublet of doublets at δ 3.96 ppm for the CH_2Cl protons, and $^3J(PH)$ 9 and 1.4 Hz (we did not previously resolve the smaller $^3J(PH)$

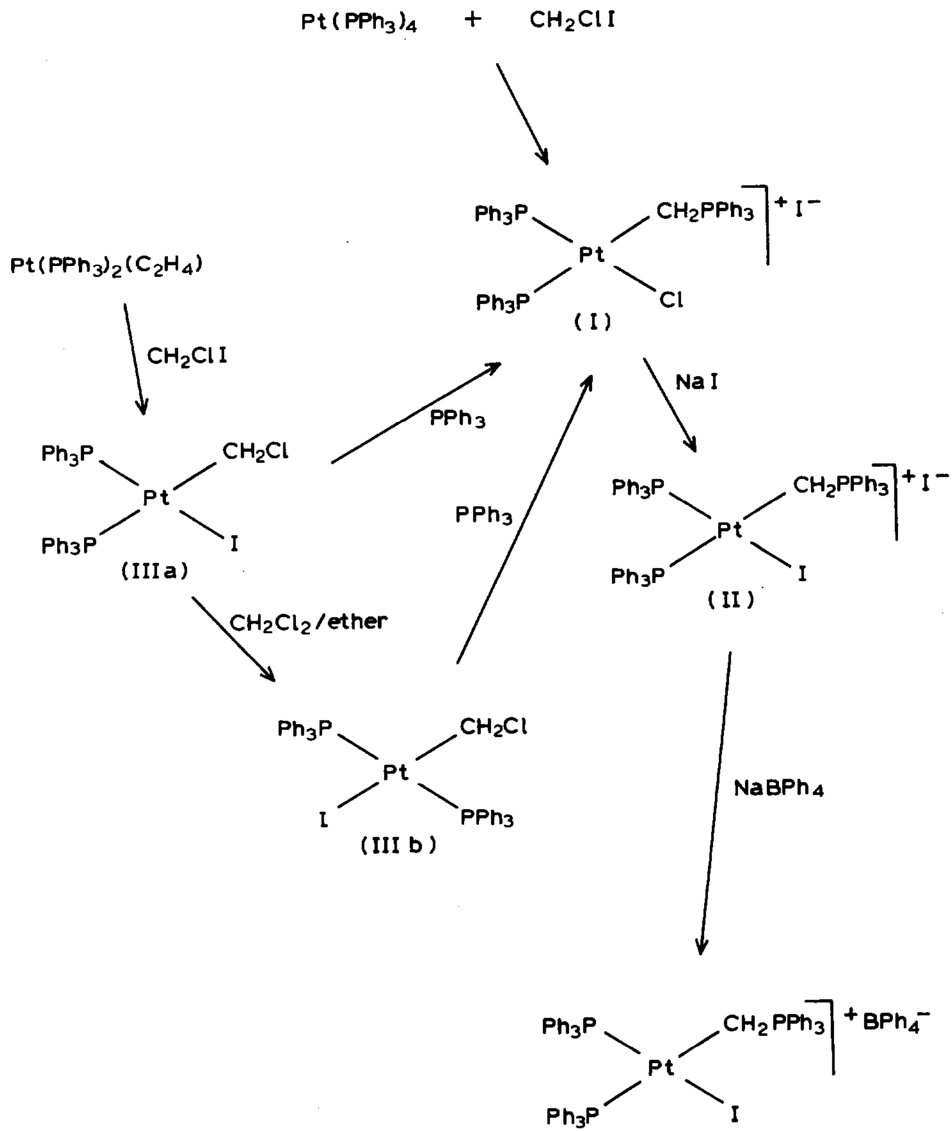

SCHEME 1

[7]). Since in IIIb ${}^3J(PH)$ is found to be 9 Hz it appears that ${}^3J(P_{trans}H) < {}^3J(P_{cis}H)$. Samples of IIIa often show a weak triplet at δ 3.06 ppm which indicates the presence of the *trans*-isomer. The intensity of the triplet increases with time and after about 4 h it is the major peak in this region of the ${}^1H$ NMR spectrum. The doublets, of the *cis*-isomer, completely disappear indicating that isomerisation of IIIa to IIIb is complete. For some samples however, complete isomerisation to the *trans*-isomer was not observed and this may be due to traces of PPh_3, for example, affecting the isomerisation. As no other peaks were observed in this region of the ${}^1H$ NMR spectrum, and because the far IR spectra for these samples, showed no

observable ν(Pt–Cl), it suggests that we did not obtain any significant amount of halogen scrambled products such as $Pt(CH_2I)Cl(PPh_3)_2$, as had previously been suggested [4]. Further evidence of isomerisation in solution was gained from the ^{31}P NMR spectrum of IIIa. Thus, immediately after making up solutions of IIIa for ^{31}P NMR measurements, two doublets, with associated platinum satellites, were observed at δ 17.59 and 14.07 ppm (relative to external 85% H_3PO_4). This spectrum we assign to the *cis*-isomer IIIa. On standing in solution over a period of several hours, the doublets of the *cis*-isomer gradually decrease in intensity and a singlet for IIIb appears at δ 23.62 ppm and then increases in intensity. After about 12 h the isomerisation to the *trans*-isomer is complete and the singlet at δ 23.62 ppm, with associated platinum satellites (^1J(PtH) 3091 Hz) is the only peak observed in the ^{31}P NMR spectrum. On standing in solution for a longer period (4–7 d) the ^{31}P NMR spectrum showed that in addition to the singlet ascribed to IIIb three new peaks formed all with Pt satellites at δ 22.41 (J(PtP) 3067 Hz), 26.72 (J(PtP) 3156 Hz), 26.18 ppm (J(PtP) 3122 Hz); these three new peaks are given in order of decreasing intensity and are all weaker than the peak due to IIIb. The ^1H NMR spectrum of a solution of IIIa after several days does not show peaks other than those of IIIb and we therefore believe that the species giving rise to the new ^{31}P NMR peaks could be due to species such as *trans*-$[PtClI(PPh_3)_2]$ formed on decomposition of IIIb. In the solid state, complicated decomposition behaviour of IIIa and IIIb is observed. For both IIIa and IIIb, new crystals form in the melts above 232°C, these then melt above 275°C and further new, fine crystals form in the melts above 290°C, which then turn black above 310°C. It thus appears that IIIa may isomerize to IIIb in the melt above 220°C then several decomposition steps take place which may represent decomposition of IIIb to species such as *trans*-$[PtClI(PPh_3)_2]$ as we suggested for the decomposition of IIIb in solution. We are carrying out further studies in order to characterize the decomposition products of IIIa and IIIb. We previously reported that IIIb was yellow [7]; we have now prepared a pure white sample of IIIb and believe that the yellow colour observed for some samples of IIIb was due to traces of impurities such as *trans*-$[PtClI(PPh_3)_2]$. This may be expected since *trans*-$[Pt(CH_2Cl)Cl(PPh_3)_2]$ has been reported to give $PtCl_2(PPh_3)_2$ as a decomposition product [3]. The reaction of either IIIa or IIIb with PPh_3 leads to the formation of the ylide complex *cis*-$[Pt(CH_2PPh_3)Cl(PPh_3)_2][I]$ thus strongly implicating the intermediacy of III in the reaction of $Pt(PPh_3)_4$ with CH_2ClI. Similarly, Scherer and Jungmann [11] have reported that reaction of *cis*/*trans*-$[Pt(CH_2Cl)Cl(PPh_3)_2]$ with PPh_3 yields *cis*-$[Pt(CH_2PPh_3)Cl(PPh_3)_2][Cl]$. The reaction of III with PPh_3 requires a novel migration of Cl from the CH_2 group to the platinum. A possible intermediate in this reaction could be the cationic species $[Pt({=}CH_2)Cl(PPh_3)_2]^+$ formed by an α-elimination. Lappert et al. [10] have previously suggested that the reaction of $Pt(PEt_3)_3$ with CH_2I_2 to give *trans*-$[Pt(CH_2PEt_3)I(PEt_3)_2][I]$ goes via an iodomethyl complex and that a similar mechanism may be operative in the reaction of $Pt(PPh_3)_4$ with CH_2ClI. There are also other examples of the formation of cationic ylide complexes from halomethyl complexes including

$$(\eta\text{-}C_5H_5)Fe(CO)_2(CH_2Cl) + PR_3 \rightarrow [(\eta\text{-}(C_5H_5)Fe(CO)_2(CH_2PR_3)]^+ \qquad [12]$$

$$(\eta\text{-}C_5H_5)Rh(PMe_3)I(CH_2I) + PR_3 \rightarrow [(\eta\text{-}(C_5H_5)Rh(PMe_3)I(CH_2PR_3)]^+ \qquad [13]$$

In order to fully characterize and confirm the presence of the ylide ligand in I, to

TABLE 1

CRYSTAL DATA, EXPERIMENTAL AND REFINEMENT PARAMETERS

	$[PtC_{55}H_{47}P_3Cl][I]\cdot CH_2Cl_2$	$[PtC_{55}H_{47}P_3I][I]\cdot CH_2Cl_2$
M_r	1243.24	1334.70
Space group	$P2_1/n$	$P2_1/n$
a	1388.6(7) pm	1379.4(7) pm
b	2026.7(10) pm	2044.4(10) pm
c	1823.9(9) pm	1840.0(9) pm
β	96.51(2)°	96.09(2)°
D_c (for $Z = 4$)	1.62 Mg m^{-3}	1.72 Mg m^{-3}
μ(Mo-K_α)	3.5 mm^{-1}	3.9 mm^{-1}
$F(000)$	2448	2592
Crystal dimensions	0.3×0.2×0.2 mm	0.4×0.32×0.08 mm
Scan mode	$\omega-2\theta$	$\omega-2\theta$
Scan width	1.0°θ	1.0°θ
Scan speed	0.033°θ s^{-1}	0.033°θ s^{-1}
Range scanned	6–40°	6–46°
Stability of standard reflections	0.99%	1.3%
Number of reflections collected	4929	5646
Number of observed reflections	3542 with I(rel) > $2\sigma I$(rel)	4333 with I(rel) > $2\sigma I$(rel)
Number of variables	190	190
$R = \Sigma\|\|F_c\| - \|F_0\|\|/\Sigma\|F_0\|$	0.075	0.071
$R_w = \Sigma w^{\frac{1}{2}}\|\|F_c\| - \|F_0\|\|/\Sigma w^{\frac{1}{2}}\|F_0\|$	0.077	0.077
Weighting scheme w	$(\sigma^2 F + 2\times10^{-3}F^2)^{-1}$	$(\sigma^2 F + 2\times10^{-3}F^2)^{-1}$

confirm the stereochemistry and to find out more about the bonding of the ylide ligand to platinum, we have determined the structures of I and II by X-ray crystallography. IR and NMR results for both I and II suggested that both complexes have the *cis*-stereochemistry. This stereochemistry is now established in the solid state by X-ray crystallography. Each of the complexes I and II crystallizes with one mole of CH_2Cl_2; this was also suggested on the basis of microanalytical data. The two complexes are isomorphous and all aspects of the atomic configurations are very similar. Crystal data, experimental and refinement parameters are given in Table 1, fractional atomic coordinates and thermal parameters in Table 2 and interatomic distances and bond angles in Table 3. The structure of II is shown in Fig. 1 and a stereoview in Fig. 2. Both complexes show essentially the same distorted square-planar arrangement of ligands around the platinum atoms (see Fig. 3 for compound I).

The large P(1)–Pt–P(2) angles of 96.5(2) and 97.0(2)° can be attributed to the bulkiness of the triphenylphosphine ligands. This is observed in other *cis*-bis(triphenylphosphine)platinum(II) complexes e.g. P–Pt–P in *cis*-$[Pt(CH_2I)I(PPh_3)_2]$ is 97.1° [4].

Pt–P bond lengths

The mean Pt–P bond length of 229(1) pm is the same as found in *cis*-$[Pt(CH_2I)I(PPh_3)_2]$ [4]. From Table 3, the Pt–P bond lengths *trans* to Cl and I are the same. Thus, any predictions on the differences in the *trans* influence of Cl and I

(*Continued on p. 264*)

TABLE 2

FRACTIONAL ATOMIC COORDINATES ($\times 10^4$) FOR $[PtC_{55}H_{47}P_3Cl][I]\cdot CH_2Cl_2$ AND $[PtC_{55}H_{47}P_3I][I]\cdot CH_2Cl_2$

Atom	x	y	z
Pt(1)	2221(1)	2139(1)	1411(1)
Cl(1A)	3291(4)	2924(2)	2060(3)
I(2)	3319(1)	473(1)	6931(1)
P(1)	1794(4)	1868(3)	2574(3)
P(2)	1162(4)	1469(3)	756(3)
P(3)	3059(4)	3138(3)	106(3)
Cl(1)	5220(9)	1176(7)	1169(6)
Cl(2)	6248(10)	188(7)	461(7)
C(1)	5891(33)	486(21)	1182(25)
C(3)	2970(14)	2322(10)	483(11)
C(111)	2949(9)	1672(6)	3126(5)
C(112)	3625(9)	1307(6)	2785(5)
C(113)	4498(9)	1119(6)	3185(5)
C(114)	4695(9)	1297(6)	3926(5)
C(115)	4020(9)	1662(6)	4267(5)
C(116)	3147(9)	1850(6)	3867(5)
C(121)	1221(10)	2519(5)	3054(7)
C(122)	972(10)	2418(5)	3765(7)
C(123)	524(10)	2921(5)	4124(7)
C(124)	324(10)	3524(5)	3771(7)
C(125)	573(10)	3625(5)	3060(7)
C(126)	1021(10)	3122(5)	2701(7)
C(131)	1020(9)	1154(5)	2725(7)
C(132)	14(9)	1227(5)	2649(7)
C(133)	−575(9)	687(5)	2761(7)
C(134)	−160(9)	75(5)	2949(7)
C(135)	846(9)	2(5)	3025(7)
C(136)	1435(9)	542(5)	2913(7)
C(211)	1185(9)	1444(6)	−251(7)
C(212)	715(9)	1947(6)	−673(7)
C(213)	730(9)	1954(6)	−1437(7)
C(214)	1214(9)	1457(6)	−1778(7)
C(215)	1683(9)	954(6)	−1355(7)
C(216)	1669(9)	947(6)	−591(7)
C(221)	−94(8)	1705(6)	789(7)
C(222)	−311(8)	2287(6)	1145(7)
C(223)	−1263(8)	2518(6)	1083(7)
C(224)	−1998(8)	2168(6)	667(7)
C(225)	−1781(8)	1586(6)	312(7)
C(226)	−829(8)	1354(6)	373(7)
C(231)	1375(7)	610(6)	1027(7)
C(232)	651(7)	154(6)	1132(7)
C(233)	898(7)	−494(6)	1334(7)
C(234)	1869(7)	−685(6)	1430(7)
C(235)	2593(7)	−229(6)	1324(7)
C(236)	2346(7)	419(6)	1123(7)
C(311)	2778(10)	3064(5)	−876(7)
C(312)	2239(10)	3551(5)	−1277(7)
C(313)	2067(10)	3506(5)	−2044(7)
C(314)	2435(10)	2974(5)	−2410(7)
C(315)	2974(10)	2487(5)	−2009(7)
C(316)	3146(10)	2532(5)	−1242(7)

TABLE 2 (continued)

Atom	*x*	*y*	*z*
C(321)	4285(9)	3468(7)	243(6)
C(322)	4581(9)	3916(7)	−267(6)
C(323)	5523(9)	4166(7)	−175(6)
C(324)	6169(9)	3968(7)	426(6)
C(325)	5872(9)	3520(7)	936(6)
C(326)	4931(9)	3270(7)	845(6)
C(331)	2239(9)	3733(5)	404(7)
C(332)	1352(9)	3515(5)	604(7)
C(333)	681(9)	3970(5)	813(7)
C(334)	896(9)	4643(5)	822(7)
C(335)	1783(9)	4860(5)	622(7)
C(336)	2455(9)	4405(5)	413(7)
Pt(1)	2239(1)	2147(1)	1416(1)
I(1)	3416(1)	3011(1)	2139(1)
I(2)	3301(1)	457(1)	6906(1)
P(1)	1779(3)	1866(2)	2556(2)
P(2)	1177(3)	1481(2)	755(2)
P(3)	3088(3)	3121(2)	88(2)
Cl(1)	5211(7)	1168(6)	1211(5)
Cl(2)	6225(9)	172(7)	487(6)
C(1)	5993(25)	532(25)	1213(24)
C(3)	2997(11)	2337(10)	496(10)
C(111)	2902(7)	1649(7)	3118(5)
C(112)	3566(7)	1265(7)	2785(5)
C(113)	4443(7)	1079(7)	3177(5)
C(114)	4657(7)	1275(7)	3903(5)
C(115)	3993(7)	1658(7)	4236(5)
C(116)	3116(7)	1845(7)	3843(5)
C(121)	1183(8)	2508(5)	3050(6)
C(122)	947(8)	2412(5)	3761(6)
C(123)	510(8)	2914(5)	4123(6)
C(124)	309(8)	3512(5)	3774(6)
C(125)	545(8)	3608(5)	3063(6)
C(126)	982(8)	3106(5)	2701(6)
C(131)	975(7)	1156(5)	2681(7)
C(132)	−34(7)	1239(5)	2610(7)
C(133)	−641(7)	710(5)	2720(7)
C(134)	−237(7)	98(5)	2900(7)
C(135)	772(7)	15(5)	2970(7)
C(136)	1378(7)	544(5)	2861(7)
C(211)	1204(8)	1464(5)	−241(6)
C(212)	708(8)	1956(5)	−653(6)
C(213)	696(8)	1958(5)	−1412(6)
C(214)	1178(8)	1467(5)	−1759(6)
C(215)	1673(8)	975(5)	−1347(6)
C(216)	1686(8)	973(5)	−588(6)
C(221)	−103(6)	1688(5)	796(6)
C(222)	−321(6)	2272(5)	1136(6)
C(223)	−1278(6)	2502(5)	1076(6)
C(224)	−2018(6)	2149(5)	676(6)
C(225)	−1800(6)	1565(5)	335(6)
C(226)	−843(6)	1335(5)	395(6)
C(231)	1404(5)	628(6)	1001(7)

continued

TABLE 2 (continued)

Atom	*x*	*y*	*z*
C(232)	693(5)	159(6)	1096(7)
C(233)	965(5)	−484(6)	1271(7)
C(234)	1948(5)	−658(6)	1351(7)
C(235)	2659(5)	−190(6)	1256(7)
C(236)	2387(5)	453(6)	1081(7)
C(311)	2776(8)	3055(5)	−890(7)
C(312)	2206(8)	3528(5)	−1279(7)
C(313)	2004(8)	3474(5)	−2036(7)
C(314)	2372(8)	2947(5)	−2403(7)
C(315)	2942(8)	2475(5)	−2014(7)
C(316)	3144(8)	2529(5)	−1257(7)
C(321)	4318(7)	3456(6)	194(6)
C(322)	4558(7)	3925(6)	−307(6)
C(323)	5492(7)	4196(6)	−244(6)
C(324)	6185(7)	3997(6)	320(6)
C(325)	5945(7)	3528(6)	821(6)
C(326)	5011(7)	3257(6)	758(6)
C(331)	2253(7)	3712(5)	401(7)
C(332)	1336(7)	3505(5)	563(7)
C(333)	671(7)	3957(5)	786(7)
C(334)	922(7)	4617(5)	847(7)
C(335)	1839(7)	4825(5)	686(7)
C(336)	2504(7)	4373(5)	462(7)

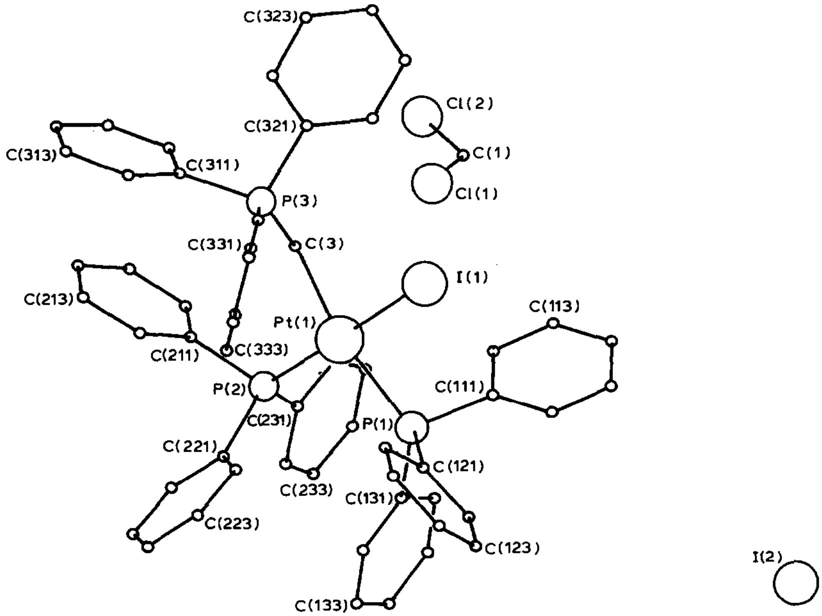

Fig. 1. The molecular structure of *cis*-[Pt(CH_2PPh_3)I(PPh_3)$_2$][I] showing the atomic labelling.

TABLE 3

SELECTED INTERATOMIC DISTANCES (pm) AND BOND ANGLES (°)

	$[PtC_{55}H_{47}P_3Cl][I]\cdot CH_2Cl_2$	$[PtC_{55}H_{47}P_3I][I]\cdot CH_2Cl_2$
Pt(1)–Cl(1A) (I(1))	240 (1)	266 (1)
Pt(1)–P(1)	233 (1)	233 (1)
Pt(1)–P(2)	225 (1)	226 (1)
Pt(1)–C(3)	212 (2)	212 (2)
C(3)–P(3)	180 (2)	178 (2)
P(1)–C(111)	184 (1)	183 (1)
P(1)–C(121)	182 (1)	184 (1)
P(1)–C(131)	184 (1)	186 (1)
P(2)–C(211)	184 (1)	184 (1)
P(2)–C(221)	182 (1)	183 (1)
P(2)–C(231)	182 (1)	182 (1)
P(3)–C(311)	180 (1)	181 (1)
P(3)–C(321)	182 (1)	182 (1)
P(3)–C(331)	178 (1)	181 (1)
C(1)–Cl(1)	168 (4)	169 (4)
C(1)–Cl(2)	158 (4)	159 (4)
P(1)–Pt(1)–Cl(1A) (I(1))	85.1(2)	85.6(1)
P(2)–Pt(1)–Cl(1A) (I(1))	175.7(2)	175.4(1)
P(2)–Pt(1)–P(1)	97.0(2)	96.5(2)
C(3)–Pt(1)–Cl(1A) (I(1))	86.9(5)	87.2(5)
C(3)–Pt(1)–P(1)	165.2(5)	166.1(4)
C(3)–Pt(1)–P(2)	91.8(5)	91.5(5)
C(111)–P(1)–Pt(1)	104.6(4)	105.9(4)
C(121)–P(1)–Pt(1)	116.0(4)	116.6(4)
C(121)–P(1)–C(111)	107.2(5)	106.9(5)
C(131)–P(1)–Pt(1)	122.3(5)	121.9(4)
C(131)–P(1)–C(111)	103.7(6)	102.8(6)
C(131)–P(1)–C(121)	101.8(6)	101.1(5)
C(211)–P(2)–Pt(1)	117.6(5)	117.9(4)
C(221)–P(2)–Pt(1)	113.3(4)	114.3(4)
C(221)–P(2)–C(211)	99.6(6)	99.6(5)
C(231)–P(2)–Pt(1)	110.9(4)	111.0(4)
C(231)–P(2)–C(211)	102.9(6)	102.1(6)
C(231)–P(2)–C(221)	111.6(6)	110.7(5)
C(311)–P(3)–C(3)	106.7(8)	109.5(7)
C(321)–P(3)–C(3)	112.9(7)	113.6(6)
C(321)–P(3)–C(311)	105.2(6)	104.8(6)
C(331)–P(3)–C(3)	115.5(7)	113.1(7)
C(331)–P(3)–C(311)	106.6(6)	105.9(5)
C(331)–P(3)–C(321)	109.2(6)	109.4(6)
P(3)–C(3)–Pt(1)	121.8(10)	124.4(10)
Cl(2)–C(1)–Cl(1)	122.3(27)	122.8(27)
C(112)–C(111)–P(1)	117.4(3)	116.4(3)
C(116)–C(111)–P(1)	122.6(3)	123.6(3)
C(122)–C(121)–P(1)	120.7(3)	121.6(3)
C(126)–C(121)–P(1)	119.3(3)	118.4(3)
C(132)–C(131)–P(1)	119.8(3)	119.8(3)
C(136)–C(131)–P(1)	120.2(3)	120.2(3)
C(212)–C(211)–P(2)	118.1(3)	117.9(3)
C(216)–C(211)–P(2)	121.9(3)	122.1(3)
C(222)–C(221)–P(2)	119.8(3)	118.2(3)
C(226)–C(221)–P(2)	119.6(3)	120.9(3)

(continued)

TABLE 3 (continued)

	$[PtC_{55}H_{47}P_3Cl][I] \cdot CH_2Cl_2$	$[PtC_{55}H_{47}P_3I][I] \cdot CH_2Cl_2$
C(232)-C(231)-P(2)	124.9(3)	125.7(3)
C(236)-C(231)-P(2)	115.1(3)	114.3(3)
C(312)-C(311)-P(3)	120.5(3)	121.4(3)
C(316)-C(311)-P(3)	119.4(3)	118.6(3)
C(322)-C(321)-P(3)	119.3(3)	118.2(3)
C(326)-C(321)-P(3)	120.7(3)	121.8(3)
C(332)-C(331)-P(3)	118.6(3)	119.2(3)
C(336)-C(331)-P(3)	121.3(3)	120.8(3)

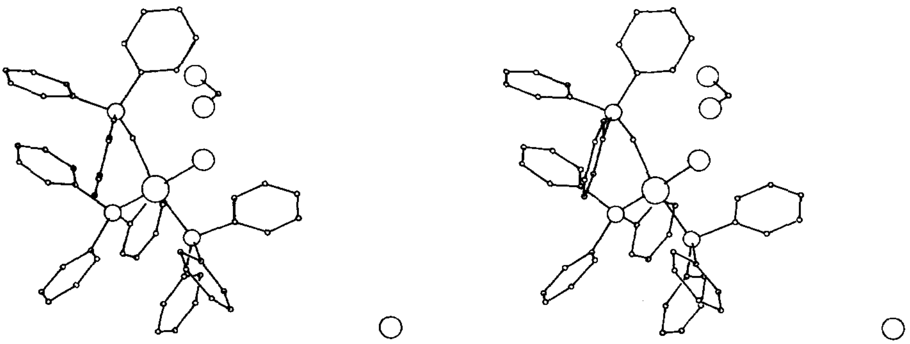

Fig. 2. A stereoview of the structure of *cis*-$[Pt(CH_2PPh_3)I(PPh_3)_2][I]$.

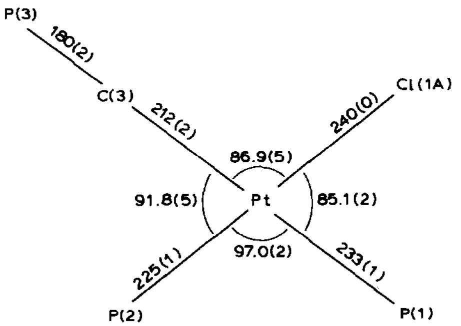

Fig. 3. The coordination about the platinum in *cis*-$[Pt(CH_2PPh_3)Cl(PPh_3)_2][I]$ showing bond distances (pm), bond angles (°) and atomic labelling.

on the basis of the Pt–P bond lengths is not possible. Also, substitution of Cl by I has little effect on the geometry of the ligands around the platinum. This is in contrast to the differences observed for the complexes *cis*-$[PtX_2(PMe_3)_2]$ (X = Cl or I) [14,15]. In both complexes I and II, the Pt–P distance *trans* to CH_2PPh_3 is longer than the Pt–P distance *trans* to Cl or I. This may be due to the strong *trans* influence of the CH_2PPh_3 group. Similarly, in *cis*-$[Pt(CH_2I)I(PPh_3)_2]$ Pt–P *trans* to CH_2I is 235.5(7) pm whereas Pt–P *trans* to I is 222.8 pm [4].

Pt–X bond lengths

The Pt–Cl distance of 240(1) pm compared well with that found in $[Pt_2Cl(CH_2PPh_3)(\mu\text{-}CH_2)(\mu\text{-}Ph_2PCH_2PPh_3)_2]^+$ of 242.4 pm [16], *trans*-$[Pt(CH_3)Cl(PPh_3)_2]$ of 243.1 pm [17] and *trans*-$[Pt(CH_2CN)Cl(PPh_3)_2]$ of 239 pm

[18]. Pt–I of 266(1) compared with 265.8 pm in *cis*-$[Pt(CH_2I)I(PPh_3)_2]$ [4] and 266.6 pm in *trans*-$[Pt(CH_2PEt_3)I(PEt_3)_2]^+$ [10].

Pt–C bond lengths

In both complexes I and II, the Pt–C bond length is 212(2) pm. This is longer than the Pt–C single bonds found in *trans*-$[Pt(CH_3)Cl(PPh_3)_2]$, 208 pm [17] and *trans*-$[Pt(CH_2CN)Cl(PPh_3)_2]$, 208 pm [18], but similar to that in *cis*-$[Pt(CH_2I)I(PPh_3)_2]$ of 208.6(24) pm [4] and in $[Pt_2Cl(CH_2PPh_3)(\mu\text{-}(CH_2)(\mu\text{-}Ph_2PCH_2PPh_2)_2]^+$ 210(2)–212(2) pm (mean of three Pt–C bonds) [16].

Pt–C(3)–P(3) bond angle

In I, this angle is 121.8(10)° and in II 124.4(10)°. These values lie near the mean for other complexes containing the CH_2PR_3 ligand. Some examples of M–C–P bond angles are 114.89(71)° in $Me_3AuCH_2PPh_3$ [19], 118(1)° in *trans*-$[Pt(CH_2PEt_3)I(PEt_3)_2]^+$ [10], 119(1)° in $[(\eta\text{-}C_5Me_5)W(CO)_3(CH_2PPh_3)]^+$ [20], 126.4(4)° in $[W(CH_2PMe_3)(CO)_2Cl(PMe_3)_3]^+$ [21] and 129(1)° in $[Pt_2Cl(CH_2PPh_3)(\mu\text{-}CH_2)(\mu\text{-}Ph_2PCH_2PPh_2)_2]^+$ [16]. All these angles are larger than the tetrahedral angle presumably as a result of steric factors.

Experimental

Microanalyses were performed by Pascher Microanalytical Laboratory, Bonn and the Microanalytical Laboratory at the University of Cape Town. IR spectra were recorded on a Perkin–Elmer model 180 spectrophotometer (Nujol mulls, with KBr discs for IR and polyethylene supports for FIR). NMR spectra were recorded on a JEOL FX 90Q or a Bruker WH90 spectrometer. Melting points were determined on a Kofler hot-stage microscope and are uncorrected. Conductivity measurements were made on approximately 10^{-3} *M* solutions in nitrobenzene using a Metrohm Konductometer E382. Reactions were routinely carried out under an atmosphere of nitrogen in Schlenk apparatus. Benzene was distilled under nitrogen from lithium aluminium hydride and acetone from anhydrous sodium sulphate. $Pt(PPh_3)_4$ [22] and $Pt(PPh_3)_2(C_2H_4)$ [23] were prepared by literature methods. CH_2ClI was prepared by the method of Miyano and Hashimoto [24] or purchased from Aldrich Chemical Co. Ltd.

Reaction of $Pt(PPh_3)_4$ with CH_2ClI

$Pt(PPh_3)_4$ (2.32 g, 1.86 mmol) was dissolved in benzene (40 ml) and the solution filtered under nitrogen to give a clear orange solution. Chloroiodomethane (0.79 g, 4.48 mmol) in benzene (5 ml) was added with stirring and the solution then allowed to stand for 6 d. In this time, a white crystalline precipitate had formed. This was filtered off, washed with benzene (3 × 5 ml) and dried to give *cis*-$[Pt(CH_2PPh_3)Cl(PPh_3)_2][I] \cdot C_6H_6$ as white microcrystals (1.78 g, 77%) m.p. 161–165°C. (Found: C, 59.03; H, 4.15; Cl, 3.37. $C_{61}H_{53}ClIP_3Pt$ calcd.: C, 59.26; H, 4.32; Cl, 2.87%). This product was recrystallized from dichloromethane/ether to give *cis*-$[Pt(CH_2PPh_3)Cl(PPh_3)_2][I] \cdot CH_2Cl_2$ as colourless crystals m.p. 166–170°C. (Found: C, 54.00; H, 4.01; Cl, 7.43; P, 6.99. $C_{56}H_{49}Cl_3IP_3Pt$ calcd.: C, 54.10; H, 3.97; Cl, 8.55; P, 7.47%). The molar conductivity of this compound was found to be 22.9 ohm^{-1} cm^2. In the IR spectrum: ν(Pt–Cl) 307s, ν(Pt–C) 572m and δ(P–C_3

deform) 543vs cm^{-1} [25]; also a band at 780s cm^{-1} (not assigned). ^{31}P NMR spectrum in CH_2Cl_2 with external H_3PO_4 (85%) as reference showed the following peaks: δ(P(3)) 31.63 ppm (d) ^3J(P(3)P(1)) 4.88 Hz with platinum satellites ^2J(PtP(3) 70.8 Hz; δ(P(2)) and δ(P(1)) 18.70 ppm (br s) with platinum satellites (d) ^1J(PtP(2)) 3987, ^2J(P(2)P(1)) 17.09 and (dd) ^1J(PtP(1)) 2244, ^2J(P(2)P(1)) 17.09, ^3J(P(3)P(1)) 4.88 Hz. The chemical shifts for P(2) and P(1) in I are coincident. ^{13}C NMR spectrum in CH_2Cl_2 shows the ylide carbon atoms as a doublet of doublets of doublets at δ 7.23 ppm to low field of TMS ^1J(P(3)C) 105, ^2J(P(2)C) 7.32, ^2J(P(1)C) 37.23 Hz (the assignments of these coupling constants are made assuming ^1J(P(1)C) $> {}^3J$(P(1)C) $> {}^2J$(P(2)C)) with platinum satellites ^1J(PtC) 576 Hz. ^{1}H NMR spectrum in CH_2Cl_2 shows a multiplet centred at δ 2.52 ppm with platinum satellites ^2J(PtH) 69 Hz. The platinum satellites show an essentially first order spectrum (doublet of doublets of doublets) with ^2J(P(3)H) $\simeq$ 14 and ^3J(P(1)H) $\simeq$ 9 Hz.

Preparation of cis-[Pt(CH_2PPh_3)I(PPh_3)$_2$][I]

Sodium iodide (4.27 g, 28.49 mmol) was added to a solution of *cis*-[Pt(CH_2PPh_3)Cl(PPh_3)$_2$][I] · CH_2Cl_2 (0.35 g, 2.28 mmol) in acetone (80 ml). The mixture was refluxed for 30 min and, after cooling, the solvent was removed under reduced pressure. The solid residue was washed well with water to give the product (0.34 g, 97%). This solid was recrystallized from dichloromethane/ether to give *cis*-[Pt(CH_2PPh_3)I(PPh_3)$_2$][I] · CH_2Cl_2 as yellow microcrystals m.p. 162–167°C. (Found: C, 50.24; H, 3.73; I, 18.89; P, 6.56. $C_{56}H_{49}Cl_2I_2P_3Pt$ calcd.: C, 50.39; H, 3.70; I, 19.01; P, 6.96%). The molar conductivity of this compound was found to be 21.9 ohm^{-1} cm^2. IR spectrum: ν(Pt–I) 171, 177 cm^{-1}, ν(P–C_3 deform) 539 [25], ν(Pt–C) 566 cm^{-1}, unassigned band at 780 cm^{-1}. ^{31}P NMR in CH_2Cl_2 δ(P(3)) 31.94 ppm (d) ^3J(P(3)P(1)) 3.66 Hz with platinum satellites (^2J(PtP(3)) 47.61 Hz; δ(P(2)) 17.44 ppm (doublet) ^2J(P(2)P(1)) 16.48 Hz with platinum satellites ^1J(PtP(2)) 3795 Hz; δ(P(1)) 11.52 ppm (dd) ^3J(P(3)P(1)) 3.66 Hz, ^2J(P(2)P(1)) 16.48 Hz with platinum satellites ^1J(PtP(1)) 2258 Hz.

Preparation of [Pt(CH_2PPh_3)I(PPh_3)$_2$][BPh_4]

[Pt(CH_2PPh_3)I(PPh_3)$_2$][I] (0.15 g, 0.11 mmol) was dissolved in methanol (22 ml) and a saturated solution of an excess of $NaBPh_4$ was added dropwise. An immediate white precipitate formed. This reaction solution was allowed to stand for 30 min and the product filtered off and washed with methanol to give the product as white microcrystals (0.10 g, 64%), m.p. 165–175°C. (Found: C, 65.65; H, 4.65. $C_{79}H_{67}BIP_2Pt$ calcd.: C, 65.79; H, 4.69%).

Reaction of Pt(PPh_3)$_2$(C_2H_4) with CH_2ClI

Pt(C_2H_4)(PPh_3)$_2$ (1.00 g, 1.34 mmol) was dissolved in a minimum of benzene (17 ml). A solution of CH_2ClI (0.50 g, 2.84 mmol) in benzene (2 ml) was added dropwise with stirring over 5 min. After 3 min, an off-white crystalline precipitate started forming. Stirring was continued for 15 min and the precipitate was then filtered, washed with hexane and dried to give white microcrystals of *cis*-[Pt(CH_2Cl)I(PPh_3)$_2$] (IIIa) (0.905 g, 75%) m.p. 216–222°C (dec.). The product was further purified by rapid recrystallisation from THF/hexane. (Found: C, 49.49; H, 3.97; Cl, 3.51; I, 14.11. $C_{37}H_{32}ClIP_2Pt$ calcd.: C, 49.60; H, 3.60; Cl, 3.96; I, 14.16%). ν(Pt–I) 190 cm^{-1}. ^{1}H NMR ($CDCl_3$) δ 3.96 ppm (dd), ^3J(PH) 9, ^3J(PH) 1.4,

^2J(PtH) 41.9 Hz. ^{31}P NMR ($CDCl_3$) (relative to 85% H_3PO_4) shows two doublets at δ 17.59 and 14.07 ppm with ^1J(PtP) of 4255 and 1748 Hz respectively and ^2J(PPtP) 17 Hz. The solvent was removed from the mother liquor of the reaction and the residue dissolved in CH_2Cl_2. Addition of hexane and cooling to −15°C gave a further crop of IIIa (0.23 g, 19%).

Conversion of cis-[Pt(CH₂Cl)I(PPh₃)₂] to trans-[Pt(CH₂Cl)I(PPh₃)₂]

cis-[Pt(CH_2Cl)I(PPh_3)$_2$] (0.107 g, 0.119 mmol) was suspended in benzene (10 ml) and heated under reflux for 1 h. The pale yellow solution was cooled to room temperature and the solvent removed under reduced pressure to give an off-white solid precipitate. This precipitate was dissolved in CH_2Cl_2 and filtered to give a pale yellow solution. The volume of solvent was reduced in a stream of nitrogen and methanol added dropwise. The solution was cooled to −15°C for 2 d and the resulting white crystalline plates were filtered and dried to give *trans*-[Pt(CH_2Cl)I(PPh_3)$_2$] (IIIb) (0.082 g, 76%) m.p. 225–232°C (dec.). (Found: C, 49.43; H, 4.03; Cl, 4.15; I, 14.00. $C_{37}H_{32}ClIP_2Pt$ calcd.: C, 49.60; H, 3.60; Cl, 3.96; I, 14.16%). ν(Pt–I) 190 cm^{-1}. ^{1}H NMR ($CDCl_3$) δ 3.06 ppm (t), ^3J(PH) 9, ^2J(PtH) 49.5 Hz, ^{31}P NMR ($CDCl_3$) δ 23.62 ppm (s), ^1J(PtP) 3091 Hz.

Reaction of cis-[Pt(CH₂Cl)I(PPh₃)₂] with PPh₃

cis-[Pt(CH_2Cl)I(PPh_3)$_2$] (0.16 g, 0.18 mmol) was dissolved in benzene (17 ml) to give a clear pale yellow solution. PPh_3 (0.10 g, 0.38 mmol) was added and the solution allowed to stand for 2.5 d. During this time, white crystals were deposited. These were filtered off and washed with hexane (2 × 5 ml) to give *cis*-[Pt(CH_2PPh_3)Cl(PPh_3)$_2$] · C_6H_6 as white crystals (0.16 g, 74%) m.p. 165–168°C. (Found: C, 59.5; H, 4.3. $C_{61}H_{53}ClIP_3Pt$ calcd.: C, 59.26; H, 4.32%). The IR spectrum in the range 4000–200 cm^{-1} was identical to that for a sample of *cis*-[Pt(CH_2PPh_3)Cl(PPh_3)$_2$][I] prepared from the reaction of Pt(PPh_3)$_4$ and CH_2Cl_2I, as was the ^{31}P NMR spectrum.

Reaction of trans-[Pt(CH₂Cl)I(PPh₃)₂] with PPh₃

trans-[Pt(CH_2Cl)I(PPh_3)$_2$] (0.20 g, 0.33 mmol) was dissolved in a minimum of benzene. The solution was warmed to 60°C for complete dissolution. PPh_3 (0.30 g, 1.14 mmol) was added and the resulting solution allowed to stand for 2 d. The white crystals which formed were filtered off and washed with hexane to give *cis*-[Pt(CH_2PPh_3)Cl(PPh_3)$_2$][I] (0.26 g, 66%) m.p. 165–168°C. The IR spectrum in the region 4000–200 cm^{-1} was identical to that of an authentic sample of *cis*-[Pt(CH_2PPh_3)Cl(PPh_3)$_2$][I] and the C and H microanalysis was also in agreement with this formulation.

X-ray data collection, structure determination and refinement for cis-[Pt(CH₂PPh₃)X(PPh₃)₂][I] · CH₂Cl₂ (X = Cl or I)

Suitable crystals were obtained by slow addition of ether to dichloromethane solutions of each of the complexes. Preliminary photographs (Cu-K_α radiation, λ 1.542 Å) revealed that both complexes crystallized in the monoclinic space group $P2_1/n$. The lattice constants were obtained by least-squares from the settings of 25 reflections measured on a Philips PW 1100 four-circle diffractometer with graphite-monochromated Mo-K_α radiation (λ 0.7107 Å).

During the data collection, three reference reflections were periodically monitored to check crystal stability. The data were corrected for Lorentz-polarisation effects, but not for absorption. The crystals of both complexes were found to be isomorphous. Using SHELX-76 [26], the Pt and coordinated Cl and I ligands were located in Patterson maps. Subsequent weighted difference syntheses yielded the positions of all the remaining non-hydrogen atoms. In the final refinements, the Pt, I, Cl and P atoms were treated anisotropically. The aromatic rings were fixed geometrically and the H atoms restrained at 108 pm from their respective C atoms, their positions being dictated by the geometry of the rings. Crystal data, experimental and refinement parameters are given in Table 1. Fractional atomic coordinates for both structures are given in Table 2. Details of thermal parameters and structure factors are available from the authors.

Acknowledgements

We thank the University of Cape Town and the CSIR for financial support. Johnson-Matthey for a generous loan of platinum salts. Martin Murray for recording some of the NMR spectra, Jon Albain for X-ray data collection and Wendy Davies, Robin Lenhoff and Cheryl Walker for experimental assistance.

References

1 See for example F.R. Hartley in G. Wilkinson, F.G.A. Stone and E.W. Abel (Eds.), Comprehensive Organometallic Chemistry, Pergamon Press, Oxford, Vol. 6, 1982, p. 518.
2 R.D. Gillard and M.F. Pilbrow, J. Chem. Soc., Dalton Trans., (1974) 2320 and refs. therein.
3 O.J. Scherer and H. Jungman, J. Organomet. Chem., 208 (1981) 153.
4 N.J. Kermode, M.F. Lappert, B.W. Skelton, A.H. White and J. Holton, J. Chem. Soc., Chem. Commun., (1981) 698.
5 C. Bartocci, A. Maldotti, S. Sostero and O. Traverso, J. Organomet. Chem., 253 (1983) 253.
6 R.A. Head, J. Chem. Soc., Dalton Trans., (1982) 1637.
7 C. Engelter, J.R. Moss, M.L. Niven, L.R. Nassimbeni, G. Reid, J. Organomet. Chem., 232 (1982) C78.
8 J.R. Moss and J.C. Spiers, J. Organomet. Chem., 182 (1979) C20.
9 W. Kaska, Coord. Chem. Rev., 48 (1983) 1.
10 N.J. Kermode, M.F. Lappert, B.W. Sketon, A.H. White and J. Holton, J. Organomet. Chem., 228 (1982) C71.
11 O.J. Scherer and H. Jungmann, Z. Naturforsch. B, 36 (1981) 1663.
12 S. Pelling, C. Botha and J.R. Moss, J. Chem. Soc., Dalton Trans., (1983) 1495.
13 H. Werner, Pure Appl. Chem., 54 (1982) 177 and references therein.
14 A. Del Pra and G. Zanotti, Cryst. Struct. Comm., 8 (1979) 737.
15 E.E. Messmer, E.L. Amma and J.A. Ibers, Inorg. Chem., 6 (1967) 725.
16 K.A. Azam, A.A. Frew, B.R. Lloyd, L. Manojlović-Muir, K.W. Muir and R.J. Puddephatt, J. Chem. Soc., Chem. Commun., (1982) 614.
17 R. Bardi and A.M. Piazzeni, Inorg. Chim. Acta, 47 (1981) 249.
18 A. Del Pra, G. Zanotti, G. Bombieri and R. Ros, Inorg. Chim. Acta, 36 (1979) 121.
19 J. Stein, J.P. Fackler, C. Paparizos and H.-W. Chen, J. Amer. Chem. Soc., 103 (1981) 2192.
20 P.M. Stretch, M.L. Niven and J.R. Moss, Inorg. Chim. Acta, 119 (1986) 177.
21 M.R. Churchill and H.J. Wasserman, Inorg. Chem., 21 (1982) 3913.
22 R. Ugo, F. Cariati and G. La Monica, Inorg. Synth., XI (1968) 105.
23 D.M. Blake and D.M. Roundhill, Inorg. Synth., XVIII (1978) 120.
24 S. Miyano and H. Hashimoto, Bull. Chem. Soc. Japan, 44 (1971) 2864.
25 S.H. Mastin, Inorg. Chem., 13 (1974) 1003.
26 G.M. Sheldrick in H. Schenk, R. Olthof-Hazekamp, H. van Koningsveld and G.C. Bassi (Eds.), Computing in Crystallography, Delft Univ. Press, Delft 1978, pp. 34–42.